Chapter 20

Reaction Behaviors of Bagasse Modified with Phthalic Anhydride in 1-Allyl-3-Methylimidazolium Chloride with Catalyst 4-Dimethylaminopyridine

Hui-Hui Wang, Xue-Qin Zhang, Yi Wei and Chuan-Fu Liu

Additional information is available at the end of the chapter

http://dx.doi.org/10.5772/65508

Abstract

The modification of lignocellulose with cyclic anhydrides could confer stronger hydrophilic properties to lignocellulose, which could be used in many industrial fields. To elucidate the modification mechanism of lignocellulose, bagasse was phthalated comparatively with its three main components in 1-allyl-3-methylimidazolium chloride (AmimCl) using 4-dimethylaminopyridine as catalyst and phthalic anhydride as acylation reagent in the present study. From FT-IR and 2D HSQC analyses, the skeleton of bagasse and the fractions were not significantly changed during phthalation in AmimCl. 2D HSQC results suggested that the reactive hydroxyls in bagasse were partially phthalated, and the reactivity of the hydroxyls in anhydroglucose units followed the order C-6 > C-2 > C-3. Similarly, the reactivity order of hydroxyls in anhydroxylose units was C-2 > C-3. For lignin, the predominant diesterification occurred during the homogeneous modification, and both aliphatic and aromatic hydroxyls were phthalated. The reactivity order of phenolic hydroxyls was S-OH > G-OH > H-OH, which was distinct from that without catalyst. In addition, it was found that the thermal stability of phthalated bagasse was affected by the disruption of cellulose crystallinity and the degradation of components. The thermal stability of the phthalated bagasse decreased upon chemical modification and regeneration.

Keywords: bagasse, phthalic anhydride, esterification, reaction behavior, 2D HSQC NMR, ^{31}P NMR, AmimCl

1. Introduction

Nowadays, the growing environmental concerns resulting from petroleum-based plastic materials and excessive use of fossil fuel have driven a strong global interest in renewable bio-based polymers and composites derived from natural resources [1, 2]. Biomass resource is one of the

most abundant, inexpensive, and currently underutilized products from agricultural and biorefinery industries [3]. Biomass resources, especially agricultural residues with great renewability, biocompatibility, and biodegradability, are directing the development of next generation of chemicals, materials, energy, and processes [4]. Therefore, it could be particularly advisable to shift society's dependence away from fossil resources to biomass resources.

Bagasse, sugar industry residues, is mainly composed of lignocellulose, which represents one of the most abundant renewable resources on earth. Chemical modification represents an efficient process to introduce new functionalities into lignocellulose. Because of the poor dissolubility of lignocellulose in common molecular solvent, the heterogeneous modification has been studied for decades. However, heterogeneous modification is always accomplished at low efficiency and nonuniformity, and accompanied with the occurrence of side reactions [5, 6]. Even worse, the solvent or reaction medium for heterogeneous modification could not be recovered after modification [7], which caused environmental pollution and wastage of resources. It is a never-ending endeavor to explore homogeneous reaction systems to compensate the deficiency of heterogeneous systems.

Fortunately, it has been found that several dual solvent systems and ionic liquids (ILs) could dissolve lignocellulose [8]. Compared with other solvent systems, ILs exhibit negligible vapor pressure, theoretically making infinite recycling possible. In addition, the high electrochemical thermal stability, nonflammability, and designability made ILs widely used in diverse fields, such as solvent for synthesis and catalysis, separation, analytical chemistry, and biomass refinery [9–11]. The bridge between lignocellulose and ILs were built by Swaltloshi et al., who reported the nonderivatizating dissolution of cellulose in BmimCl [12]. In 2007, it was reported that woods with different hardness could be readily dissolved in various imidazium-based ILs under mild conditions [13, 14], which opened a new window of opportunities in homogeneous functionalization of lignocellulose. Since then, the chemical modification of lignocellulose in ILs has been expanding fast. Due to the existence of abundant hydroxyls in lignocellulose, the modification of lignocellulose with carboxylic anhydride, acid chloride, and isocyanides could be achieved using ILs as reaction media [15].

The chemical modification of lignocellulose with linear carboxylic acid anhydrides or acid chloride can produce the corresponding carboxylic acid or HCl as a by-product. However, the modification of lignocellulose with dicarboxylic acid anhydride is an effective process and can attach carboxyl groups onto lignocellulose. The attachment of carboxyl group can greatly improve the compatibility between modified lignocellulose and other polymer materials by producing new chemical linkages and the effect of hydrogen bonds [16]. Besides, the introduction of carbonyl group could also increase the hydrophilicity [17], achieve ion exchange [18], and remove heavy mental ion [19]. Our previous works showed that the homogeneous chemical modification of the isolated cellulose from bagasse with succinic anhydride and phthalic anhydride without catalyst could be achieved, and the optimal reaction conditions (reaction temperature 90°C and reaction time 90 min) for preparing modified cellulose with maximum degree of substitution (DS) were also screened [20, 21]. In 2010, Li et al. reported chemical modification of cellulose in BmimCl with catalyst DMAP could remarkably improve the DS of modified products [22]. However, the structural parameters of lignocellulosic derivatives were

http://dx.doi.org/10.5772/65508

complex and difficult to control due to the complicated mixture of cell wall components. Therefore, it is very essential to elucidate the modification mechanism of lignocellulose to produce tunable materials directly from lignocellulose, although some simple investigations have been published. Especially, the application of catalyst DMAP could obviously increase the degree of substitution of lignocellulose modified with cyclic anhydride, which is beneficial to produce polymer composites based on esterified lignocellulose. As far as the authors are aware, there have been no reports of the detailed structural changes of lignocellulose during the homogeneous phthalation with catalyst DMAP. We therefore investigated the reaction behaviors of lignocellulose during the homogenous phthalation with catalyst DMAP.

In the present study, bagasse was modified with phthalic anhydride with catalyst DMAP in AmimCl. Three main components cellulose, hemicelluloses, and lignin were isolated from bagasse, and were phthalated under the same conditions to elucidate the modification mechanism. The physicochemical properties of phthalated samples were characterized by FT-IR, CP/MAS ^{13}C NMR, ^{1}H NMR, liquid-state ^{13}C NMR, and 2D HSQC NMR. The thermal stability of the unmodified, regenerated, and modified materials was also investigated using TG.

2. Material and methods

2.1. Materials

Bagasse was obtained from a local factory (Jiangmen, China). It was dried in sunlight and then cut into small pieces. The cut bagasse was ground and screened to prepare 40–60 mesh size particles (450–900 μm). The dried ground samples were dewaxed with toluene-ethanol (2:1 v/v) and then dried in a cabinet oven with air circulation at 50°C for 24 h [15]. Ionic liquid AmimCl was purchased from the Shanghai Cheng Jie Chemical Co., Ltd. and used as received. All other chemicals used were of analytical grade and purchased from Guangzhou Chemical Reagent Factory (Guangzhou, China).

2.2. Isolation of cellulose, hemicelluloses and lignin from bagasse

Cellulose and hemicelluloses were isolated according to the previous literatures [21, 23]. Briefly, the extractive-free bagasse was delignified at 75°C for 2 h with sodium chlorite at pH 3.8–4.0, followed by the extraction with 10% NaOH with the ratio of solid to liquid at 1:20 g/mL for 10 h at room temperature (four times). The solid residues were filtered out, washed thoroughly with distilled water, then washed with ethanol and dried in an oven with air circulation at 50°C for 24 h to obtain cellulose. The filtrate from NaOH extraction (the first time) was neutralized, concentrated, and transferred into three volumes of 95% ethanol with agitation. The precipitates were filtered out, washed with 70% ethanol, and freeze-dried to obtain hemicelluloses.

Lignin was isolated from the extractive-free bagasse according to the previous literatures [24, 25]. The obtained crude lignin with high content of carbohydrates was purified as follows: dried crude lignin (1 g) was dissolved in 2 mL of acetone/water (9:1, v/v) in a beaker. The obtained lignin solution was added dropwise into 200 mL of distilled water with stirring, and the resulted suspension was further centrifuged. The obtained solid residues were washed

with distilled water (thrice, total 90 mL), and then freeze-dried. The dried residues were dissolved into 2 mL of 1,2-dichloroethane/ethanol (2:1, v/v). The obtained solution was added dropwise into 200 mL of anhydrous ether in a beaker with stirring at room temperature, and the resulted suspension was further agitated for 30 min. The obtained suspension was centrifuged, and the solid residues was washed with anhydrous ether (thrice, total 90 mL) and freeze-dried.

2.3. Homogeneous phthalation of bagasse and the isolated fractions (cellulose, hemicelluloses and lignin)

The homogeneous phthalation of bagasse and its isolated fractions was performed according to the previous literature [26]. The extractive-free ground bagasse (12 g) was first finely ball-milled for 4 h in a planetary mill (Grinder BM4, China, Beijing) at 400 rpm using two 500 mL ZrO2 jars (500 g, 1 cm diameter). Cellulose isolated from bagasse was also ball-milled for 4 h under the same conditions, while hemicelluloses and lignin were directly used in the present study.

Typically, the prepared materials (0.2 g) was added to 10 g of AmimCl at room temperature under nitrogen atmosphere for 5 min and heated at 90°C under stirring for 4 h to obtain a clear solution. Phthalic anhydride (the weight ratio of phthalic anhydride to material, 4:1) and DMAP (the weight ratio of DMAP to phthalic anhydride, 5%) were added to the solution. The flask was continuously purged with nitrogen atmosphere for 5 min. The reaction was performed at 90°C for 90 min with agitation. Subsequently, the resulted solution was precipitated with ethanol (99 wt%, 200 mL) under agitation. The suspension was further stirred for 24 h. The solid residues were filtered out, washed with ethanol (three times, total 600 mL) to remove unreacted phthalic anhydride, catalyst DMAP, and AmimCl, and free-dried for further characterization.

2.4. Determination of WPG and DS

WPG [15] was calculated according to Eq. (1):

$$WPG = \frac{M_1 - M_0}{M_0} \times 100 \tag{1}$$

where M_0 and M_1 are the vacuum-dried weights of the bagasse or fractions before and after chemical modification, respectively.

The phthalation degree of phthalated samples was evaluated by DS, according to Eq. (2):

$$DS = \frac{n_{OH'}}{n_{OH}} \times 100 \tag{2}$$

where n_{OH}' is the substituted hydroxyls contents, and n_{OH} is the hydroxyl content of unmodified sample.

The substituted hydroxyl content of the phthalated samples was determined based on the equivalent volume of known molarity NaOH and HCl by back-titration method [21]. A known

http://dx.doi.org/10.5772/65508

weight of the sample was dissolved in 10 mL 0.1 mol/L NaOH. The excess of NaOH was back-titrated with 0.025 mol/L HCl by using automatic potentiometric titrator, and the final pH of end titration point was set as 7.0. The titration was repeated three times, and the average value of HCl volume was used as the calculations of the substituted hydroxyl content according to Eq. (3):

$$n_{OH'} = \frac{c_1 V_1 - c_2 V_2}{2} \times \frac{1000}{m} \tag{3}$$

where n_{OH}' is the substituted hydroxyls contents, m (g) is the dry weight of sample analyzed, c_1 (mol/L) is the molarity of NaOH, V_1 (mL) is the volume of NaOH, c_2 (mol/L) is the molarity of HCl, and V_2 (mL) is the equivalent volume of known molarity HCl.

Based on the assumption that the cellulose and hemicelluloses are composed of AGU and AXU, respectively, the theoretical hydroxyl content of unmodified cellulose and hemicelluloses were calculated from their macromolecular structure according to Eqs. (4) and (5), respectively. The total hydroxyl content of unmodified lignin was 6.31 mmol/g by ^{31}P NMR analysis. The hydroxyl content of unmodified bagasse was calculated from Eq. (6), according to the contents of cellulose, hemicelluloses, and lignin in the extractive-free bagasse:

$$n_C = \frac{1000}{162} \times 3 \tag{4}$$

where n_C (mmol/g) is the theoretical hydroxyl content of unmodified cellulose, 162 g/mol is the molar mass of AGU, and 3 is the number of hydroxyl groups on each AGU, and

$$n_H = \frac{1000}{132} \times 2 \tag{5}$$

where n_H (mmol/g) is the theoretical hydroxyl content of unmodified hemicelluloses, 132 g/mol is the molar mass of AXU, and 2 is the number of hydroxyl groups on each AXU, and

$$n_B = n_C \times 44.85 + n_H \times 33.13 + n_L \times 19.24 \tag{6}$$

where n_B and n_L (mmol/g) are the hydroxyl contents of unmodified bagasse and lignin, respectively, and 44.85%, 33.13%, and 19.14% are the contents of cellulose, hemicelluloses, and lignin, respectively, in the extractive-free bagasse according to the standard NREL methods.

2.5. Characterization

FT-IR spectra were collected on an FT-IR spectrophotometer (Nicolet 510) using a KBr disk containing approximately 1% finely ground samples. Thirty-two scans were taken for each sample with a resolution of 2 cm^{-1} in transmittance mode in the range of 4000–400 cm^{-1}.

^{1}H NMR, ^{13}C NMR, ^{31}P NMR, and 2D HSQC spectra were recorded on Bruker AV-III HD 600 spectrometer (Germany). The ^{1}H NMR spectra were recorded at 298.0 K from the dried

samples (40 mg) dissolved in 0.5 mL DMSO-d_6. The detailed collecting and processing parameters for ^{1}H NMR analysis were as follows: number of scans, 16; receiver gain, 31; acquisition time, 2.7263 s; relaxation delay, 1.0 s; pulse width, 11.0 s; spectra frequency, 600.17 Hz; and spectra width, 12019.2 Hz.

For CP/MAS ^{13}C NMR analysis, dried samples (200 mg) were tested at 303.0 K. The detailed collecting and processing parameters were as follows: number of scans, 2000; receiver gain, 567; acquisition time, 0.0344 s; relaxation delay, 1.5 s; pulse width, 4.55 s; spectra frequency, 100.61Hz; and spectra width, 29761.9 Hz.

For liquid-state ^{13}C NMR analysis, dried samples (40 mg) was dissolved in 0.5 mL DMSO-d_6 at 298.0 K, the detailed collecting and processing parameters were as follows: number of scans, 15,000; receiver gain, 1290; acquisition time, 1.2583 s; relaxation delay, 1.5 s; pulse width, 12.00 s; spectra frequency, 100.61 Hz; and spectra width, 26041.7 Hz.

For 2D HSQC NMR analysis, the spectra were acquired using 40 mg samples in the 0.5 mL DMSO-d_6 at 299.9 K. The detailed collecting and processing parameters were as follows: number of scans, 16; receiver gain, 187; acquisition time, 0.1420 s; relaxation delay, 2.0 s; pulse width, 11.0 s; spectra frequency, 600.17/150.91 Hz; and spectra width, 7211.51/24875.6 Hz.

The hydroxyls contents of lignin samples were determined by ^{31}P NMR spectroscopy, according to the reported method [25]. The detailed collecting and processing parameters were as follows: number of scans, 300; receiver gain, 187; acquisition time, 0.3408 s; relaxation delay, 2.0 s; pulse width, 12.0 s; spectra frequency, 242.95 Hz; and spectra width, 96,153.8 Hz.

TG of samples was performed on a simultaneous thermal analyzer (SDT Q600, TA Instrument). The sample weighted between 8 and 10 mg. The scans were first run from room temperature to 100°C, were equilibrated at 100°C for 5 min, and then were cooled to 40°C at the cooling rate of 20°C/min. The scans were again heated from 40°C to 700°C at the heating rate of 10°C/min under nitrogen flow.

3. Results and discussion

3.1. Homogeneous phthalation of bagasse and its fractions

The reaction behaviors of bagasse during homogeneous phthalation in AmimCl were investigated comparatively with the isolated fractions under the same conditions. The contents of cellulose, hemicelluloses, and lignin in the extractive-free bagasse were determined as 44.85%, 33.13%, and 19.14%, respectively, according to the standard NREL methods [27].

As shown in **Table 1**, the DS of phthalated cellulose, hemicelluloses, and lignin were 19.88%, 13.67%, and 27.10%, respectively, indicating the reactivity of lignin was the highest among the three main components during bagasse homogeneous modification in AmimCl. The DS of phthalated bagasse (10.80%) was lower than phthalated fractions, which was probably due to the complicated linkages between bagasse fractions. Besides, the WPG of phthalated cellulose, hemicelluloses, and lignin were 17.04%, 5.98%, and -49.70%, respectively, suggesting that the

http://dx.doi.org/10.5772/65508

	Phthalation conditions				n_{OH}' (mmol/g)	DS (%)	WPG (%)
Sample no	Molar ratio[a]	DMAP[b]	Time (min)	Temperature (°C)			
B_s	4:1	5%	90	60	1.57	10.80	-10.51%
C_s	4:1	5%	90	60	3.68	19.88	17.04%
H_s	4:1	5%	90	60	2.07	13.67	5.98%
L_s	4:1	5%	90	60	1.71	27.10	-49.70%

[a]Represents the weight ratio (w/w) of phthalic anhydride/materials.
[b]Represents the dosage of catalyst dimethylaminopyridine (DMAP) by weight ratio (w/w).
B_s, C_s, H_s, and L_s represent the phthalated bagasse, cellulose, hemicelluloses, and lignin, respectively.

Table 1. The substituted hydroxyl content, weight percent gain, and degree of substitution of samples.

significant degradation of lignin occurred during homogeneous phthalation. The WPG of phthalated bagasse was -10.51%, probably resulting from the degradation of lignin during bagasse homogeneous modification.

3.2. ^{31}P NMR analysis

To investigate the detailed information of lignin hydroxyls during homogeneous modification, ^{31}P NMR spectroscopy was applied in the present study to quantify the hydroxyl contents of lignin samples [28, 29]. The ^{31}P NMR spectra of unmodified lignin (L_o, spectrum a) and phthalated lignin (L_s, spectrum b) are shown in **Figure 1**. According to the reported literatures [30, 31], the assignments of signals in ^{31}P NMR spectra were as followed: international standard (IS), 145.50–144.80 ppm; aliphatic OH, 149.50–145.50 ppm; phenolic S-OH, 143.50–142.50 ppm; phenolic G-OH, 140.00–138.50 ppm; phenolic H-OH 138.00–137.50 ppm; COOH, 135.50–134.50 ppm.

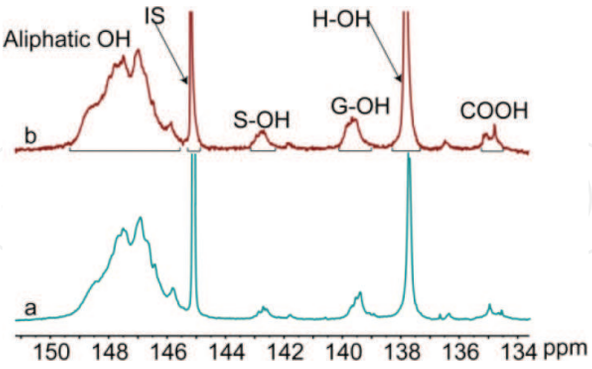

Figure 1. ^{31}P NMR spectra of unmodified lignin (L_o, spectrum a) and phthalated lignin (L_s, spectrum b).

The hydroxyl contents of unmodified and phthalated lignin are present in **Table 2**, and the decreased percentages of lignin hydroxyls are shown in **Figure 2**. After phthalation, the aliphatic hydroxyl content decreased from 4.71 mmol/g in unmodified lignin to 3.33 mmol/g in phthalated lignin, and the total phenolic hydroxyl content was also reduced from 1.60 (L_o) to 1.27 mmol/g (L_s). These results indicated that both aromatic and phenolic hydroxyls were

phthalated during lignin modification in AmimCl. Besides, the total hydroxyl content of lignin decreased from 6.31 (L_o) to 4.60 mmol/g (L_s), while the carboxyl content slightly increased from 0.08 (L_o) to 0.09 (L_s) mmol/g. The result suggested that the predominant diester form [32] during lignin homogeneous modification in AmimCl. For lignin phenolic hydroxyls, the content of phenolic S-OH decreased from 0.16 to 0.09 mmol/g after phthalation; the content of phenolic G-OH decreased from 0.40 (L_o) to 0.25 (L_s) mmol/g; the decrease in the content of phenolic H-OH from 1.04 (L_r) to 0.93 (L_s) mmol/g was also observed. These results indicated phenolic S-, G-, and H-OH were phthalated during lignin modification in AmimCl.

Sample	L_o	L_s
Aliphatic OH (mmol/g)	4.71	3.33
Phenolic OH (mmol/g)	1.60	1.27
S-OH (mmol/g)	0.16	0.09
G-OH (mmol/g)	0.40	0.25
H-OH (mmol/g)	1.04	0.93
COOH (mmol/g)	0.08	0.09
S/G ratio (mmol/g)	0.40	0.38

Table 2. The hydroxyl contents of lignin samples.

As shown in **Figure 2(a)**, the decreased percentage of aromatic hydroxyls was higher than that of phenolic hydroxyls, indicating the higher reactivity of aliphatic hydroxyls during lignin homogeneous phthalation. For phenolic hydroxyls, the decreased percentage of phenolic S-OH, G-OH, and H-OH were present (**Figure 2b**). Therefore, the phthalation reactivity of phenolic hydroxyls followed the order of S-OH > G-OH > H-OH.

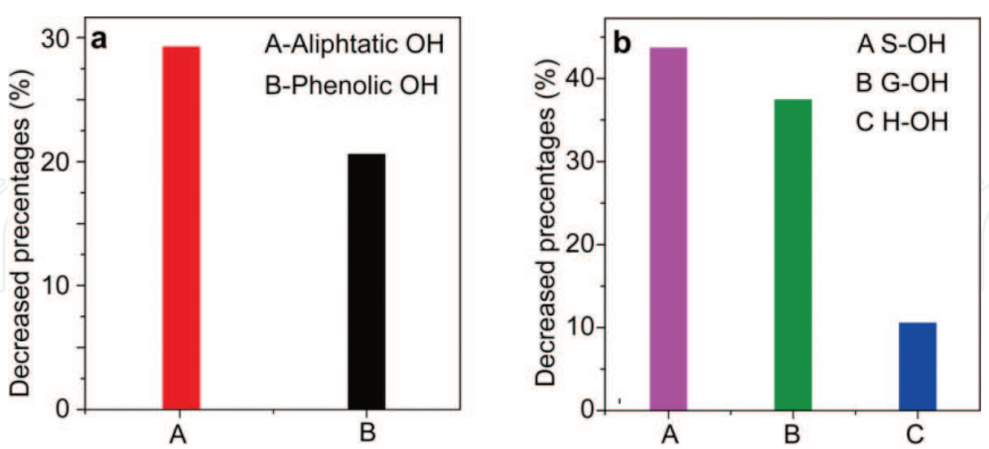

Figure 2. The decreased percentages of lignin hydroxyls.

3.3. FT-IR

The FT-IR spectra of unmodified cellulose (C_o, spectrum a), regenerated cellulose (C_r, spectrum b), and phthalated cellulose (C_s, spectrum c) are shown in **Figure 3**. The absorbance at 3433,

http://dx.doi.org/10.5772/65508

2895, 1646, 1376, 1165, and 1057 cm^{-1} were associated with unmodified cellulose [20]. These peaks present in regenerated and phthalated cellulose indicated that the skeleton of cellulose was stable during cellulose dissolution and modification in AmimCl. Compared with the spectrum of unmodified cellulose, the spectrum of the phthalated cellulose (spectrum c) provides evidence of phthalation by showing the presence of three new bands at 1718, 1580, and 749 cm^{-1} [21], corresponding to the stretching of carbonyl group, antisymmetric stretching of carboxylic anions, and the out-of-plane C-H bending of ortho disubstituted benzene, respectively. In addition, the intensity of peak at 1057 cm^{-1} for C-O-C stretching in spectrum c slightly decreased indicating the degradation of cellulose macromolecules during dissolution and modification. This degradation was also reported in the previous literature [21].

Figure 4 illustrates the FT-IR spectra of unmodified hemicelluloses (spectrum a), regenerated hemicelluloses (spectrum b), and phthalated hemicelluloses (spectrum c). Similarly, the

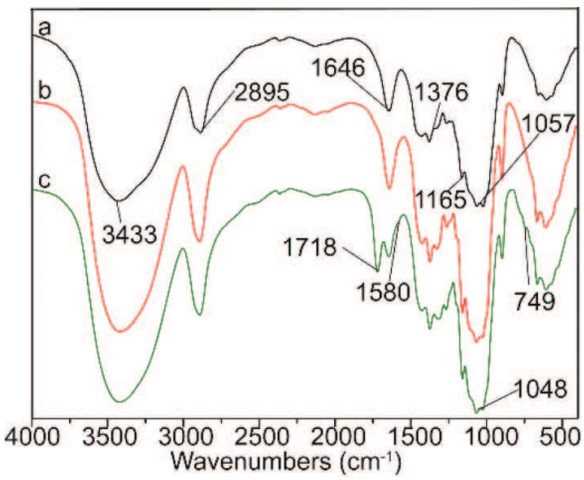

Figure 3. FT-IR spectra of unmodified cellulose (C_o, spectrum a), regenerated cellulose (C_r, spectrum b), and phthalated cellulose (C_s, spectrum c).

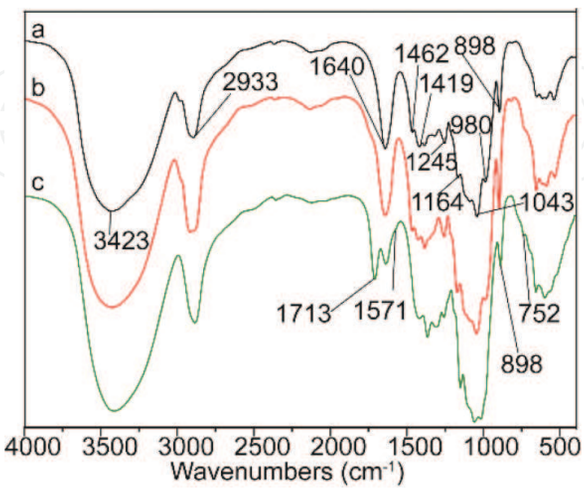

Figure 4. FT-IR spectra of unmodified hemicelluloses (H_o, spectrum a), regenerated hemicelluloses (H_r, spectrum b), and phthalated hemicelluloses (H_s, spectrum c).

skeleton of hemicelluloses remained unchanged after dissolution and modification in AmimCl. Compared with unmodified hemicelluloses, the new bands at 1713, 1571, and 752 cm^{-1} in phthalated hemicelluloses indicated the phthalation of hemicelluloses [33].

The FT-IR spectra of unmodified lignin (spectrum a), regenerated lignin (spectrum b), and phthalated lignin (spectrum c) are present in **Figure 5**. The bands at 3418, 2930, 1692, 1504, 1595, 1267, 1118, 1031, 824, and 747 cm^{-1} are related to unmodified lignin [34, 35]. Similar to cellulose and hemicelluloses, the skeleton of lignin was also stable after dissolution and modification in AmimCl. Compared with unmodified lignin, the intensity of bands at 1702 and 748 cm^{-1} in phthalated lignin obviously increased, suggesting the occurrence of esterification between lignin and phthalic anhydride [36].

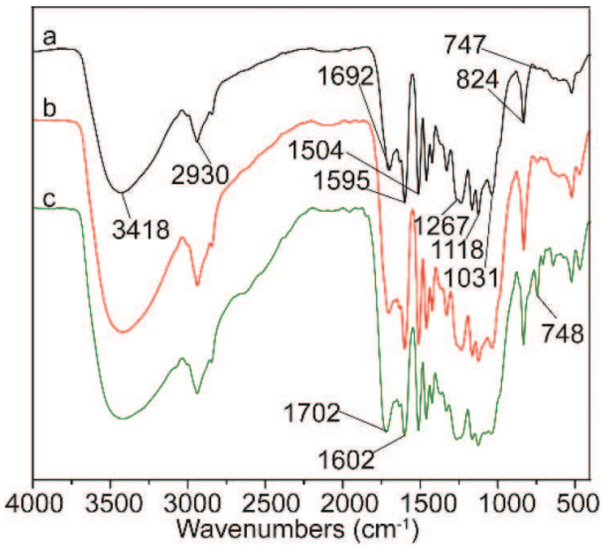

Figure 5. FT-IR spectra of unmodified lignin (L_o, spectrum a), regenerated lignin (L_r, spectrum b), and phthalated lignin (L_s, spectrum c).

FT-IR spectra of unmodified bagasse (B_o, spectrum a), regenerated bagasse (B_r, spectrum b), and phthalated bagasse (B_s, spectrum c) are shown in **Figure 6**. The bands were assigned according to the previous literature [37]. The peaks at 1605, 1515, 1375, and 897 cm^{-1} remained predominant in modified bagasse, suggesting the skeleton of bagasse fractions were unchanged during bagasse homogeneous modification in ionic liquid AmimCl [15]. The intensities of the peak at 1725 and 744 cm^{-1} increased after modification, providing the direct evidence of esterification between phthalic anhydride and bagasse. In conclusion, the phthalation of bagasse and its fractions occurred during homogeneous modification according to FT-IR analyses.

3.4. NMR analysis

3.4.1. Solid-state ^{13}C NMR of bagasse

The poor dissolubility of bagasse samples in DMSO-d_6 made high-resolution liquid-state 2D HSQC NMR spectroscopy impossible, and CP/MAS ^{13}C NMR spectroscopy was applied for bagasse samples analysis, as shown in **Figure 7**. The signals in CP/MAS ^{13}C NMR spectra were assigned based on the reported literatures [15, 21]. The signals at 191.2, 170.5, and 130.5 ppm

http://dx.doi.org/10.5772/65508

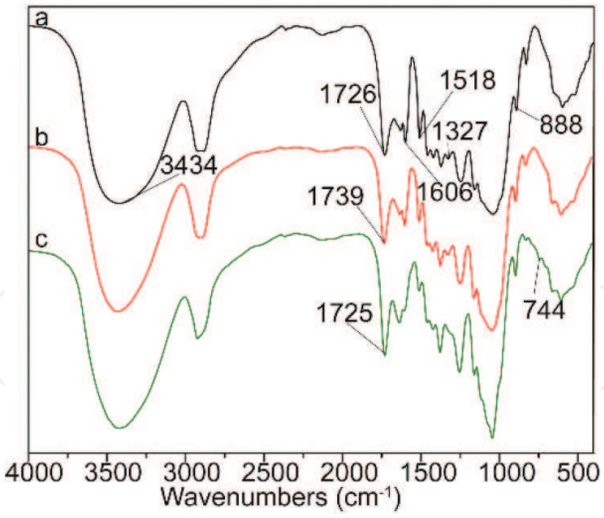

Figure 6. FT-IR spectra of unmodified bagasse (B_o, spectrum a), regenerated bagasse (B_r, spectrum b), and phthalated bagasse (B_s, spectrum c).

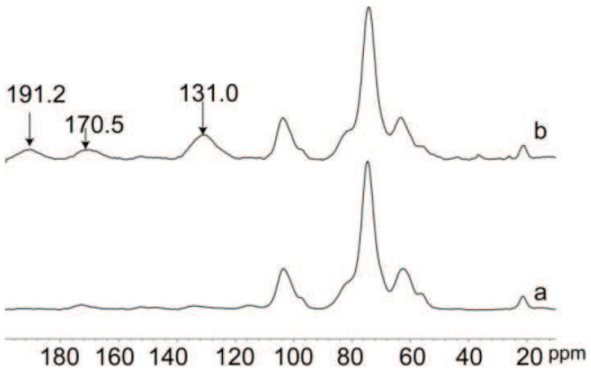

Figure 7. Solid-state ^{13}C NMR spectra of unmodified bagasse (B_o, spectrum a) and phthalated bagasse (B_s, spectrum b).

correspond to benzene ring, carbonyl group, and carboxylic groups, respectively, in phthalated bagasse. Compared with unmodified bagasse, the intensities of the three signals in phthalated bagasse remarkably increased, indicating the attachment of phthaloyl group onto bagasse.

The signals between 60 and 105 ppm relate to the carbons of carbohydrates. The chemical shifts and intensities of signals in this region remained basically unchanged, indicating the carbon skeleton of bagasse polysaccharides (cellulose and hemicelluloses) was stable during homogeneous modification, which was consistent with the results from FT-IR. Due to the low resolution of CP/MAS ^{13}C NMR spectroscopy, the detailed information of bagasse fractions during homogeneous phthalation need to be further revealed with 2D HSQC NMR spectroscopy.

3.4.2. Detailed reaction behaviors of cellulose during homogeneous phthalation

The HSQC spectra of unmodified cellulose (spectrum a) and phthalated cellulose (spectrum b) are present in **Figure 8**. The primary correlations of cellulose were well assigned, as reported in the previous literatures [20, 21]. The cross-peaks of cellulose were clearly observed in **Figure 8(a)** and **(b)** at 73.49/3.06 [C-C_2 (C_2/H_2)], 75.33/3.36 [C-C_3 (C_3/H_3)], 80.85/3.33 [C-C_4 (C_4/H_4)], 77.14/

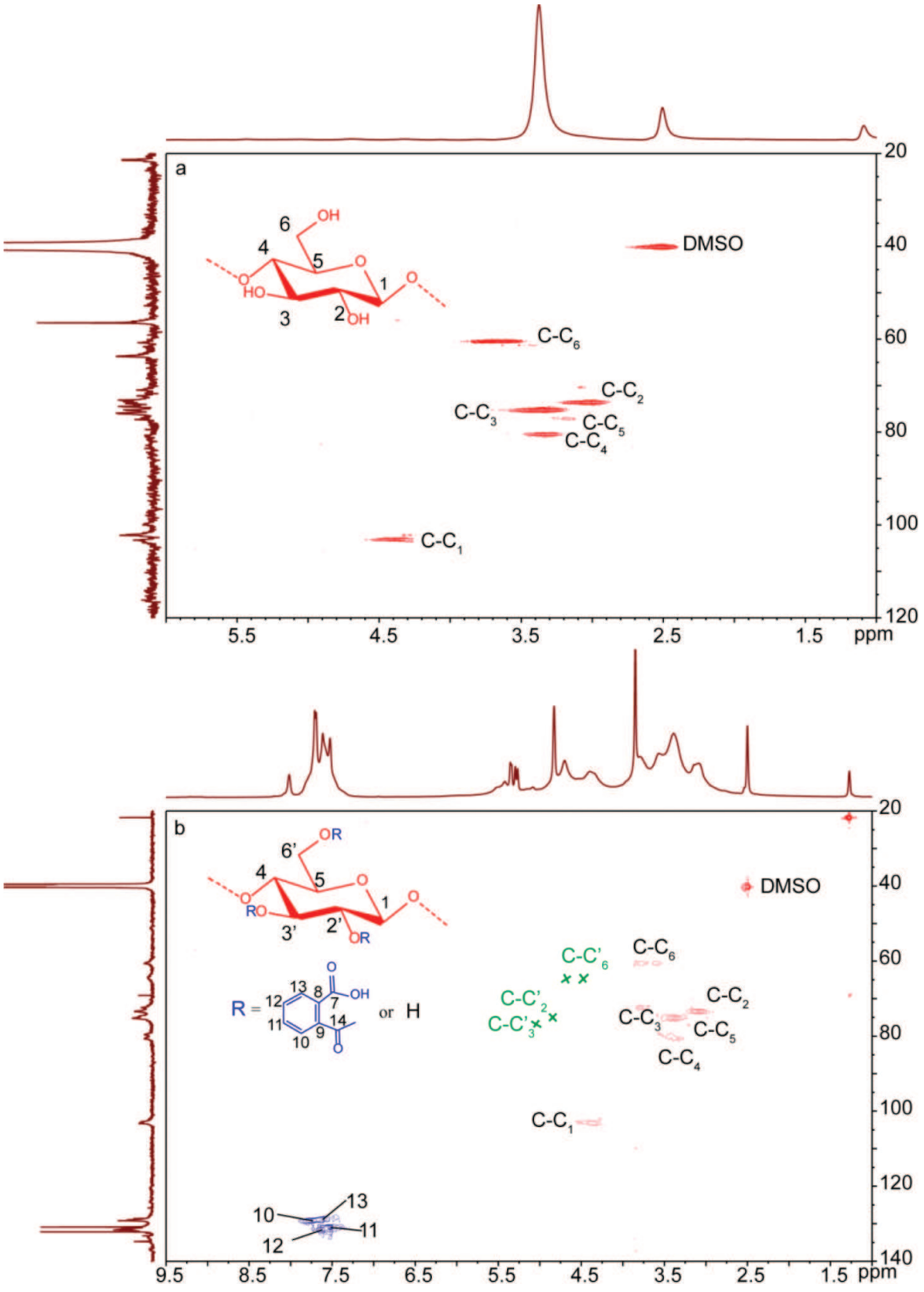

Figure 8. 2D HSQC spectra of unmodified cellulose (C_o, spectrum a) and phthalated cellulose (C_s, spectrum b).

3.18 [C-C_5 (C_5/H_5)], and 103.44/4.33 [C-C_1 (C_1/H_1)] ppm; the two C-C_6 (C_6/H_6) peaks were also distinctively located at 60.77/3.79 and 60.77/3.58 ppm, respectively. These results confirmed that the skeleton of cellulose was stable during homogeneous phthalation in AmimCl, consistent with the FT-IR analysis.

The cross-peaks at 131.49/7.62, 131.11/7.52, 129.43/7.78, and 128.94/7.61 ppm were associated with C_{10}/H_{10}, C_{11}/H_{11}, C_{12}/H_{12}, and C_{13}/H_{13} in the aryl group of phthalated cellulose, respectively. The presence of these peaks in phthalated cellulose confirmed the attachment of phthaloyl group onto cellulose. More importantly, two peaks from substituted C-6 in AGU C-C_6′ (C_6/H_6) appeared at 64.39/4.39 and 64.50/4.67 ppm, and peaks from substituted C-2 [C-C_2′ (C_2/H_2)] and C-3 [C-C_3′ (C_3/H_3)] in AGU were located at 74.32/4.60 and 75.30/4.83 ppm, respectively. These results suggested the successful phthalation of hydroxyls at C-6, C-2, and C-3 positions in AGU. The DS of hydroxyls on different positions could be evaluated upon the integral area of the characteristic substituted correlations. By integration, the DS of C_6-OH, C_2-OH, and C_3-OH in AGU were 12.05, 2.54, and 1.84%, respectively. Therefore, the DS of hydroxyls in AGU followed the order C-6 > C-2 > C-3. The phthalated cellulose was previously prepared under the similar experimental conditions without catalyst in our laboratory, and the DS of hydroxyls at C-6, C-2, and C-3 positions were 6.30, 2.01, and 0% in AGU, respectively. By contrast, it could be concluded that the addition of catalyst DMAP could improve the uniformity and DS of phthalated cellulose.

3.4.3. Detailed reaction behaviors of hemicelluloses during homogeneous phthalation

The 2D HSQC spectra of unmodified hemicelluloses (spectrum a) and phthalated hemicelluloses (spectrum b) are present in **Figure 9**. According to the previous literatures [38, 39], the correlations of xylan were at 102.12/4.25 [X-C_1 (C_1/H_1)], 73.39/3.03 [X-C_2 (C_2/H_2)], 74.60/3.23 [X-C_3 (C_3/H_3)], and 75.84/3.4 [X-C_4 (C_4/H_4)] ppm, respectively, and the cross-peaks from X-C_5 (C_5/H_5) appeared at 63.59/3.16 and 63.59/3.86 ppm in both unmodified and phthalated hemicelluloses. Besides, the cross-peaks of arabinose were also well resolved at 107.76/5.24 [A-C_1 (C_1/H_1)], 86.62/3.89[A-C_4 (C_4/H_4)], 81.32/3.76[A-C_2 (C_2/H_2)], 78.32/3.57 [A-C_3 (C_3/H_3)], and 62.13/3.40 [A-C_5 (C_5/H_5)] ppm, respectively. These results indicated that the hemicelluloses isolated from bagasse were mainly composed of arabinose and xylan, consistent with the previous literatures [25, 27]. Compared with unmodified hemicelluloses, the cross-peaks at 128.81/7.66, 129.34/7.76, 130.99/7.51, and 131.31/7.63 ppm were for C_{12}/H_{12}, C_9/H_9, C_{10}/H_{10}, and C_{11}/H_{11}, respectively, in the phthaloyl group of phthalated hemicelluloses. These results further confirmed the occurrence of the esterification between hemicelluloses and phthalic anhydride during homogeneous modification in AmimCl. The cross-peaks at 74.95/4.70 and 76.58/5.02 ppm relate to the phthalated hydroxyls at C-2 and C-3 positions in AXU. The DS of hydroxyls at C-2 and C-3 positions in AXU were 3.56 and 1.54% by integral evaluation, indicating the higher reactivity of C_2-OH in AXU during hemicelluloses homogeneous phthalation.

3.4.4. Detailed reaction behaviors of lignin during homogeneous phthalation

The 2D HSQC NMR spectra of unmodified lignin (spectrum a) and phthalated lignin (spectrum b) are illustrated in **Figure 10**, and the structure of identified lignin subunits with

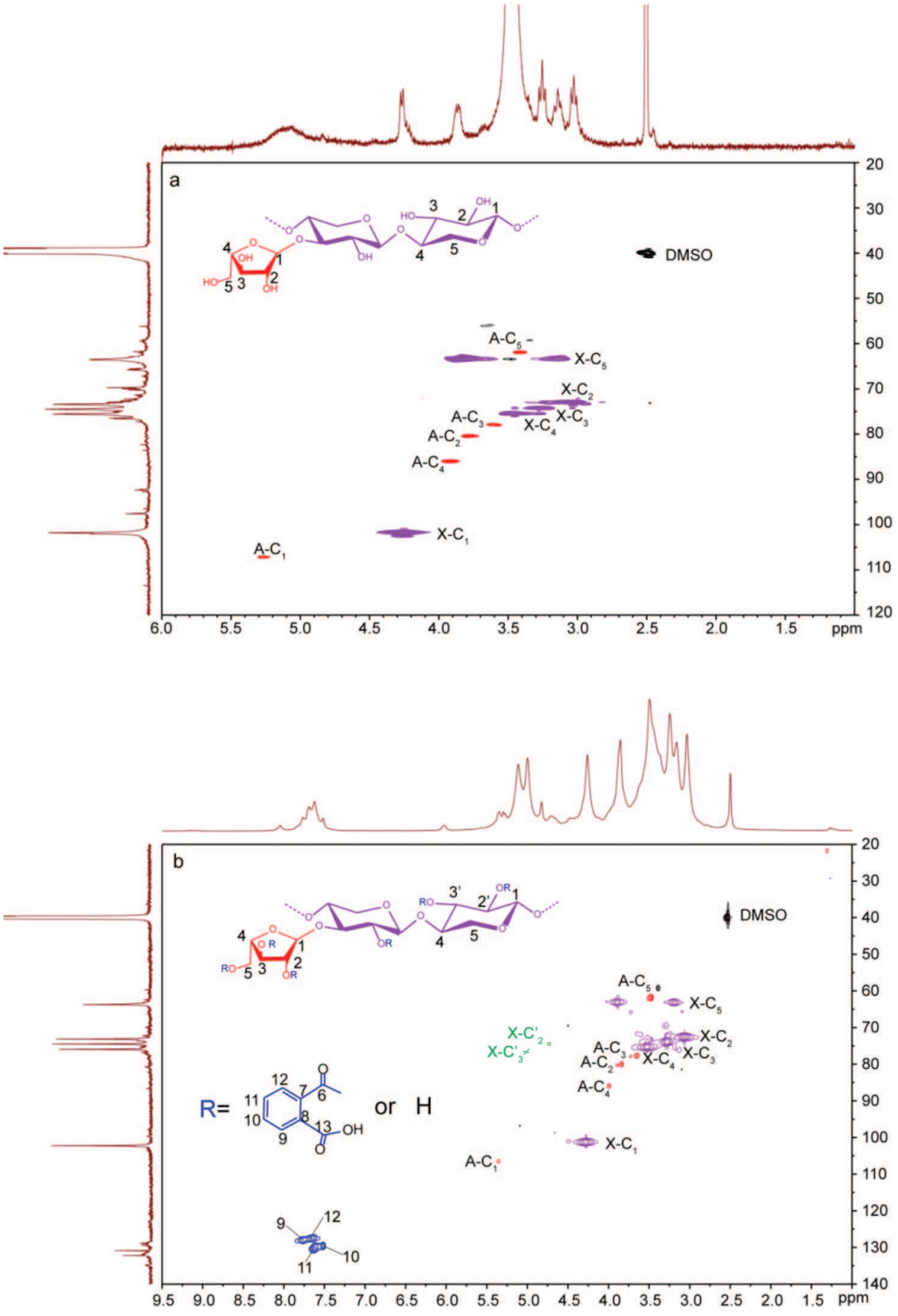

Figure 9. 2D HSQC spectra of unmodified hemicelluloses (H_o, spectrum a) and phthalated hemicelluloses (H_s, spectrum b).

http://dx.doi.org/10.5772/65508

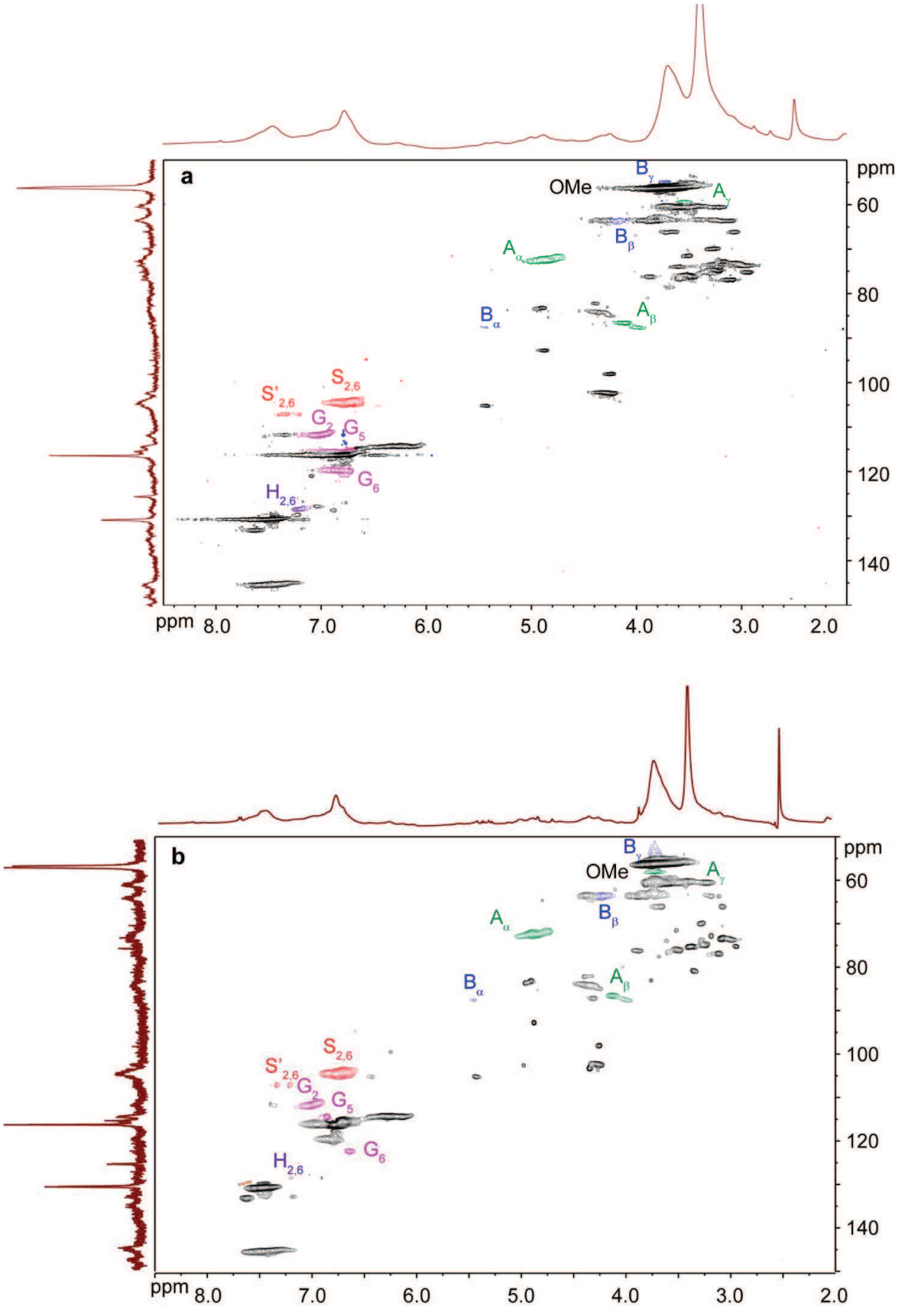

Figure 10. 2D HSQC spectra of unmodified lignin (L_o, spectrum a) and phthalated lignin (L_s, spectrum b).

hydroxyls are shown in **Figure 11**, including aryl ether (β-O-4′, A), phenylcoumaran (β-5′, B), guaiacyl unit (G-unit, C), syringyl unit (S-unit, S), and *p*-hydrophenyl unit (H-unit, H). According to the previous publications [24, 25], the correlations of these signals were well assigned. The cross-peaks from S-units $C_{2,6}/H_{2,6}$ was at 104.68/6.72 ppm, and the signals for C_α-oxidized S-units (S') appeared at δ_C/δ_H 107.15/7.34 ppm. The cross-peaks originated from G-units were well distinguished: C_2/H_2 (δ_C/δ_H 111.69/7.00 ppm), C_5/H_5 (δ_C/δ_H 115.33/6.71 ppm), and C_6/H_6 (δ_C/δ_H 119.75/6.80 ppm). The $C_{2,6}/H_{2,6}$ correlations in H-units at δ_C/δ_H 118.66/7.20 ppm was also observed. For lignin side-chains, lignin substructures with hydroxyls were also well recognized. The C_α/H_α, C_β/H_β (linked to G/H units), C_β/H_β (linked to S units), and C_γ/H_γ correlations in β-*O*-4′ linkages were at δ_C/δ_H 72.43/4.84, 84.16/4.35, 86.69/4.09, and 60.35/3.48 ppm, respectively. In addition, phenylcoumaran (β-5′, substructure B) appeared in noticeable amounts as indicated by the C_α/H_α, C_β/H_β, and C_γ/H_γ correlations at δ_C/δ_H 87.67/5.43, 55.36/3.70, and 63.50/4.21 ppm, respectively.

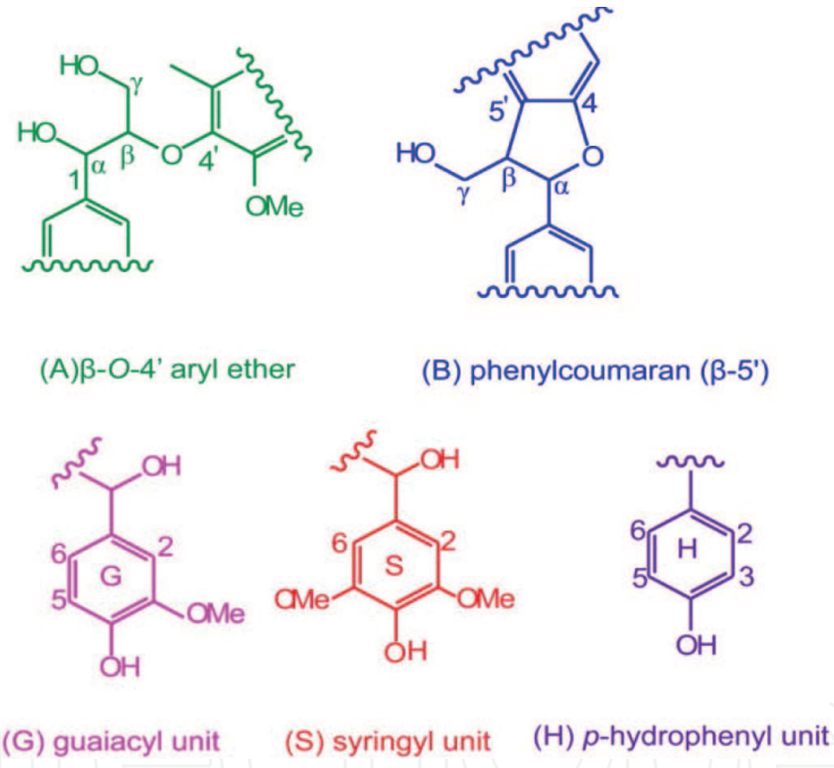

Figure 11. The structure of lignin subunits.

The relative quantities of the primary substructures were calculated according to the previous literatures [40, 41]. The aromatic lignin S-, G-, and H-units were expressed as a fraction of 100%, and the relative molar quantities of aryl ether, phenylcoumaran were expressed as a percentage of the total aromatic S-, G-, and H-units. The detailed information of quantitative lignin substructures calculated from HSQC spectra are listed in **Table 3**.

After phthalation, the content of aryl ether increased from 57.80/100Ar (L_o) to 58.33/100Ar (L_s), and the content of phenylcoumaran also increased from 2.76/100Ar (L_o) to 3.13/100Ar (L_s). These increases were probably due to the decreased intensity of $C_{2,6}/H_{2,6}$ correlations from

Sample	L_o	L_s
Aliphatic percentages of (S+G+H)		
Aryl ether (A)	57.80/100Ar	58.33/100Ar
Phenylcoumaran (B)	2.76/100Ar	3.13/100Ar
Aromatic molar percentages (S+G+H)		
Syringyl (S)	49.54%	57.81%
Guaiacyl (G)	45.78%	37.50%
p-hydroxyphenyl (H)	4.59%	4.69%
S/G	1.08	1.54

Table 3. Quantitative information of unmodified lignin (L_o) and phthalated lignin (L_s) determined with 2D HSQC NMR.

aromatic units resulting from the condensation of lignin [41] during the homogeneous phthalation. The relative percentages of G-units decreased from 45.78% to 37.50%, while the increases in the relative percentage of S- and H-units were observed. This result suggested that the G-units were easily degraded during lignin homogeneous modification [42, 43]. Besides, the increase in the S/G ratio from 1.08 (L_o) to 1.54 (L_s) further confirmed the degradation of G-units during lignin homogeneous modification.

3.5. Thermal analysis

In the present study, the effect of dissolution, regeneration, and modification in AmimCl on the thermal stability of samples was investigated by comparing unmodified, regenerated, and phthalated samples. **Figure 12** illustrates the TG curves of cellulose (A), hemicelluloses (B), lignin (C), and bagasse (D), respectively.

The onset and midpoint degradation temperature of regenerated cellulose were higher than those of unmodified cellulose, indicating the improved thermal stability after dissolution and regeneration in IL. This was probably because cellulose fractions with low molecular weight could not be regenerated from IL [15]. As shown in **Table 4**, the onset and midpoint degradation temperature of phthalated cellulose were lower than those of regenerated cellulose, suggesting the thermal stability of phthalated cellulose decreased after homogeneous modification. The decreased thermal stability of phthalated cellulose was probably due to partial hydrolysis, degradation of cellulose, and decrystallization of crystalline cellulose macromolecules [21].

Similar to cellulose, the thermal stability of regenerated hemicelluloses were slightly higher than that of unmodified hemicelluloses, probably resulting from the loss of hemicellulosic fractions with low molecular weights during dissolution and regeneration in AmimCl. Compared with regenerated hemicelluloses, the onset and midpoint degradation temperature of phthalated hemicelluloses decreased to 212 and 265°C, respectively, indicating the decreased thermal stability of phthalated hemicelluloses after homogeneous modification. This decrease was also possibly resulted from the degradation of hemicelluloses during homogeneous modification [44].

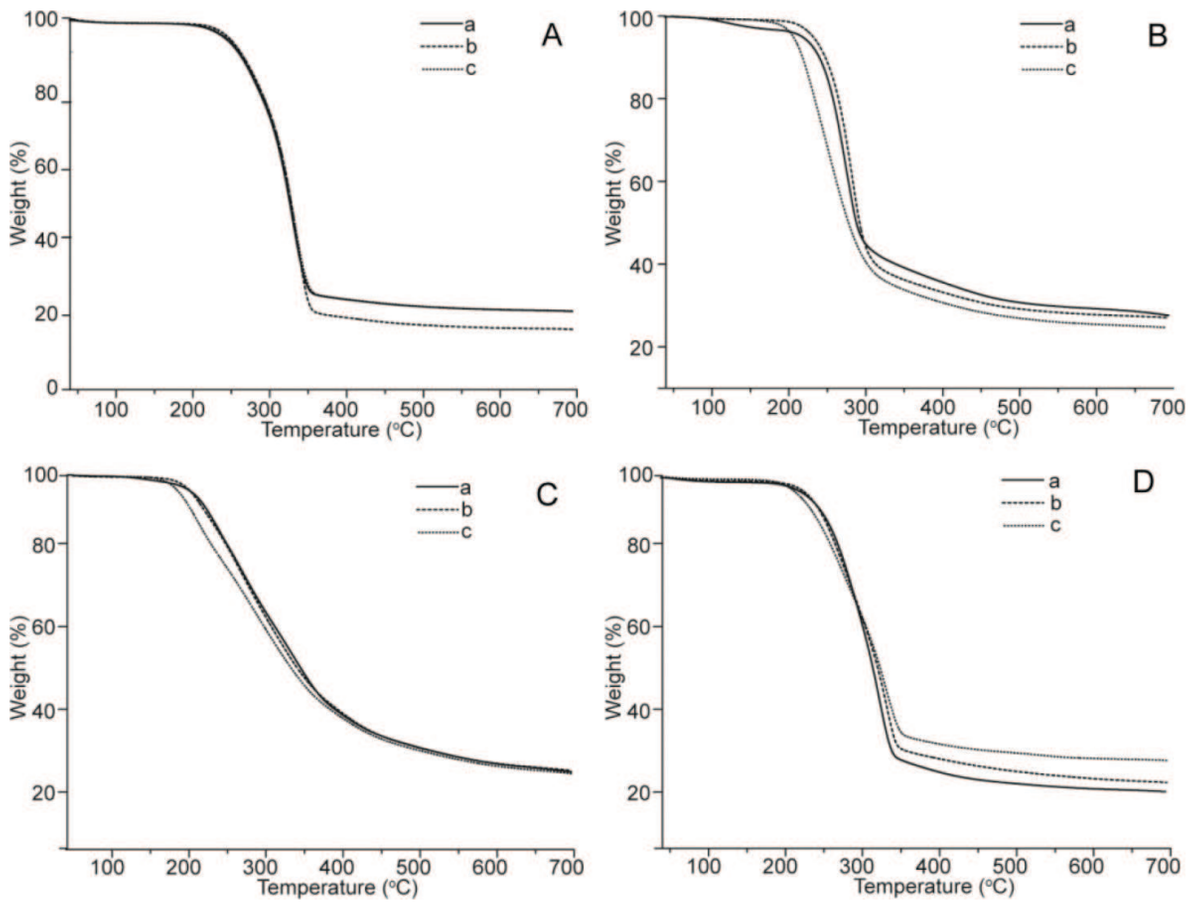

Figure 12. TG curves of cellulose (A), hemicelluloses (B), lignin (C), and bagasse (D), respectively. The curves a, b, and c represent unmodified, regenerated, and phthalated samples, respectively.

Sample	Onset T (°C)	Midpoint T (°C)
C_o	279	315
C_r	292	320
C_s	282	319
H_o	240	281
H_r	243	282
H_s	212	265
L_o	200	358
L_r	196	345
L_s	174	345
B_o	256	305
B_r	248	302
B_s	244	304

Table 4. The onset and midpoint degradation temperature of samples.

The onset and midpoint degradation temperature of regenerated lignin were both lower than those of unmodified lignin, as listed in **Table 4**, indicating the decreased thermal stability of lignin after dissolution and regenerating. Compared with regenerated lignin, the thermal stability of phthalated lignin after homogeneous modification was also decreased. This decrease was probably resulted from the degradation of lignin during dissolution, regeneration, and modification in AmimCl.

For bagasse, the thermal stability of bagasse samples decreased after dissolution and regeneration in ionic liquid AmimCl. This was probably resulted from the degradation of lignin during dissolution and regeneration. Compared with regenerated bagasse, the onset degradation temperature of phthalated bagasse decreased, while the midpoint degradation temperature of phthalated bagasse increased. These results suggested the thermal stability of lignocellulose was affected by the loss of fractions with low molecular weights and the degradation of phthalated samples. The former led to the increase in the thermal stability, while the later resulted in the decreased thermal stability of phthalated lignocellulose.

4. Conclusions

The phthalation of bagasse and its fractions occurred during homogeneous modification in AmimCl, and the reactivity of the three main components followed the order: lignin > cellulose > hemicelluloses. The FT-IR and NMR analyses suggested the skeleton of bagasse remained stable during dissolution, regeneration, and modification; the reactivity of hydroxyls in AGU followed the order: C-6 > C-2 > C-3; and the reactivity order in AXU was as follows: C-2 > C-3. For lignin, both aromatic and phenolic hydroxyls were phthalated; the reactivity of aromatic hydroxyls was higher than phenolic hydroxyls; and the reactivity order of lignin phenolic hydroxyls was as follows: S-OH > G-OH > H-OH. The thermal stability of modified lignocellulose was affected by the disruption of cellulose crystallinity and the degradation reaction of the modified components.

Acknowledgments

This work was financially supported by the National Natural Science Foundation of China (31170550, 31170555), the Fundamental Research Funds for the Central Universities (2014ZG0046), and the National Program for Support of Top-notch Young Professionals.

Nomenclature

AmimCl	1-allyl-3-methylimidazolium chloride
DMAP	4-dimethylaminopyridine
ILs	ionic liquids

DS	degree of substitution
FT-IR	Fourier transform infrared resonance
CP/MAS	solid-state cross polarization/magnetic angle spinning
NMR	nuclear magnetic resonance
2D HSQC	two dimensional heteronuclear single quantum correlation
AGU	anhydroglucose units
AXU	anhydroxylose units
S	syringyl
G	guaiacyl
H	*p*-hydroxyphenyl
DMSO-d_6	perdeutero-dimethylsulfoxide
BmimCl	1-butyl-3-methylimicazium chloride
TG	thermogravimetric analysis
WPG	weight percentage gain

Author details

Hui-Hui Wang, Xue-Qin Zhang, Yi Wei and Chuan-Fu Liu*

*Address all correspondence to: chfliu@scut.edu.cn

State Key Laboratory of Pulp and Paper Engineering, South China University of Technology, Guangzhou, PR China

References

[1] Nagarajan V, Mohanty AK, Misra M. Sustainable green composites: Value addition to agricultural residues and perennial grasses. ACS Sustainable Chemistry & Engineering. 2013;**1:**325–333. DOI: 10.1021/sc300084z

[2] Ragauskas AJ, Williams CK, Davison BH, Britovsek G, Cairney J, Eckert CA, Frederick WJ, Hallett JP, Leak DJ, Liotta CL. The path forward for biofuels and biomaterials. Science. 2006;**311:**484–489. DOI: 10.1126/science.1114736

[3] Liam B, Philip O. Biofuels from microalgae—A review of technologies for production, processing, and extractions of biofuels and co-products. Renewable and Sustainable Energy Reviews. 2010;**14:**557–577. DOI: 10.1016/j.rser.2009.10.009

[4] Minjares-Fuentes R, Femenia A, Garau MC, Candelas-Cadillo MG, Simal S, Rosselló C. Ultrasound-assisted extraction of hemicelluloses from grape pomace using response surface methodology. Carbohydrate Polymers. 2016;**138:**180–191. DOI: 10.1016/j.carbpol.2015.11.045

[5] Massimo B, Giovanna F, Mariastella S, Antonino L. Surface chemical modification of natural cellulose fibers. Journal of Applied Polymer Science. 2002;**83:**38–45. DOI: 10.1002/app.2229

[6] Freire CSR, Silvestre AJD, Neto CP, Belgacem MN, Gandini A. Controlled heterogeneous modification of cellulose fibers with fatty acids: Effect of reaction conditions on the extent of esterification and fiber properties. Journal of Applied Polymer Science. 2006;**100:**1093–1102. DOI: 10.1002/app.23454

[7] Viera RGP, Rodrigues Filho G, de Assunção RMN, Meireles CdS, Vieira JG, de Oliveira GS. Synthesis and characterization of methylcellulose from sugar cane bagasse cellulose. Carbohydrate Polymers. 2007;**67:**182–189. DOI: 10.1016/j.carbpol.2006.05.007

[8] Fasching M, Schröder P, Wollboldt RP, Weber HK, Sixta H. A new and facile method for isolation of lignin from wood based on complete wood dissolution. Holzforschung. 2008;**62:**15–23. DOI: 10.1515/HF.2008.003

[9] Sheldon RA. Green solvents for sustainable organic synthesis: State of the art. Green Chemistry. 2005;**7:**267–278. DOI: 10.1039/b418069k

[10] Olivier-Bourbigou H, Magna L, Morvan D. Ionic liquids and catalysis: Recent progress from knowledge to applications. Applied Catalysis A: General. 2010;**373:**1–56. DOI: 10.1016/j.apcata.2009.10.008

[11] Zakrzewska ME, Bogel-Łukasik E, Bogel-Łukasik R. Ionic liquid-mediated formation of 5-hydroxymethylfurfural? A promising biomass-derived building block. Chemical Reviews. 2010;**111:**397–417. DOI: 10.1021/cr100171a

[12] Swatloski RP, Spear SK, Holbrey JD, Rogers RD. Dissolution of cellose with ionic liquids. Journal of the American Chemical Society. 2002;**124:**4974–4975. DOI: 10.1021/ja025790m

[13] Kilpeläinen I, Xie HB, King AS, Granstrom M, Heikkinen S, Argyropoulos DS. Dissolution of wood in ionic liquids. Journal of Agricultural and Food Chemistry. 2007;**55:**9142–9148. DOI: 10.1021/jf071692e

[14] Fort DA, Remsing RC, Swatloski RP, Moyna P, Moyna G, Rogers RD. Can ionic liquids dissolve wood? Processing and analysis of lignocellulosic materials with 1-n-butyl-3-methylimidazolium chloride. Green Chemistry. 2007;**9:**63–69. DOI: 10.1039/b607614a

[15] Chen MJ, Chen CY, Liu CF, Sun RC. Homogeneous modification of sugarcane bagasse with maleic anhydride in 1-butyl-3-methylimidazolium chloride without any catalysts. Industrial Crops and Products. 2013;**46:**380–385. DOI: 10.1016/j.indcrop.2013.02.023

[16] Ibrahim MM, Dufresne A, El-Zawawy WK, Agblevor FA. Banana fibers and microfibrils as lignocellulosic reinforcements in polymer composites. Carbohydrate Polymers. 2010;**81:**811–819. DOI: 10.1016/j.carbpol.2010.03.057

[17] Xie HB, King A, Kilpelainen I, Granstrom M, Argyropoulos DS. Thorough chemical modification of wood-based lignocellulosic materials in ionic liquids. Biomacromolecules. 2007;**8:**3740–3748. DOI: 10.1021/bm700679s

[18] Nada AA, Hassan ML. Ion exchange properties of carboxylated bagasse. Journal of Applied Polymer Science. 2006;**102:**1399–1404. DOI: 10.1002/app.24255

[19] Anirudhan TS, Radhakrishnan PG. Chromium (III) removal from water and wastewater using a carboxylate-functionalized cation exchanger prepared from a lignocellulosic residue. Journal of Colloid and Interface Science. 2007;**316:**268–276. DOI: 10.1016/j.jcis.2007.08.051

[20] Liu CF, Sun RC, Zhang AP, Ren JL, Wang XA, Qin MH, Chao ZN, Luo W. Homogeneous modification of sugarcane bagasse cellulose with succinic anhydride using a ionic liquid as reaction medium. Carbohydrate Research. 2007;**342:**919–926. DOI: 10.1016/j.carres.2007.02.006

[21] Liu CF, Sun RC, Zhang AP, Qin MH, Ren JL, Wang XA. Preparation and characterization of phthalated cellulose derivatives in room-temperature ionic liquid without catalysts. Journal of Agricultural and Food Chemistry. 2007;**55:**2399–2406. DOI: 10.1021/jf062876g

[22] Li WY, Lan W, Chen D, Liu CF, Sun RC. DMAP-catalyzed phthalylation of cellulose with phthalic anhydride in [bmim] Cl. BioResources. 2011;**6:**2375–2385.

[23] Peng F, Ren JL, Xu F, Bian J, Peng P, Sun RC. Fractional study of alkali-soluble hemicelluloses obtained by graded ethanol precipitation from sugar cane bagasse. Journal of Agricultural and Food Chemistry. 2009;**58:**1768–1776. DOI: 10.1021/jf9033255

[24] Moghaddam L, Zhang Z, Wellard RM, Bartley JP, O'Hara IM, Doherty WOS. Characterisation of lignins isolated from sugarcane bagasse pretreated with acidified ethylene glycol and ionic liquids. Biomass and Bioenergy. 2014;**70:**498–512. DOI: 10.1016/j.biombioe.2014.07.030

[25] Zhang AP, Liu CF, Sun RC, Xie J. Extraction, purification, and characterization of lignin fractions from sugarcane bagasse. BioResources. 2013;**8:**1604–1614.

[26] Chen MJ, Shi QS. Transforming sugarcane bagasse into bioplastics via homogeneous modification with phthalic anhydride in ionic liquid. ACS Sustainable Chemistry & Engineering. 2015;**3:**2510–2515. DOI: 10.1021/acssuschemeng.5b00685

[27] Lan W, Liu CF, Sun RC. Fractionation of bagasse into cellulose, hemicelluloses, and lignin with ionic liquid treatment followed by alkaline extraction. Journal of Agricultural and Food Chemistry. 2011;**59:**8691–8701. DOI: 10.1021/jf201508g

[28] Argyropoulos DS. Quantitative phosphorus-31 NMR analysis of lignins, a new tool for the lignin chemist. Journal of Wood Chemistry and Technology. 1994;**14:**45–63.

[29] Crestini C, Argyropoulos DS. Structural analysis of wheat straw lignin by quantitative 31P and 2D NMR spectroscopy. The occurrence of ester bonds and α-O-4 substructures. Journal of Agricultural and Food Chemistry. 1997;**45:**1212–1219. DOI: 10.1021/jf960568k

[30] Pu YQ, Cao SL, Ragauskas AJ. Application of quantitative 31P NMR in biomass lignin and biofuel precursors characterization. Energy & Environmental Science. 2011;**4:**3154–3166. DOI: 10.1039/c1ee01201k

[31] Jasiukaityte E, Kunaver M, Crestini C. Lignin behaviour during wood liquefaction—Characterization by quantitative ^{31}P, ^{13}C NMR and size-exclusion chromatography. Catalysis Today. 2010;**156:**23–30. DOI: 10.1016/j.cattod.2010.02.001

[32] Vaidya AA, Gaugler M, Smith DA. Green route to modification of wood waste, cellulose and hemicellulose using reactive extrusion. Carbohydrate Polymers. 2016;**136:**1238–1250. DOI: 10.1016/j.carbpol.2015.10.033

[33] Peng XW, Ren JL, Sun RC. Homogeneous esterification of xylan-rich hemicelluloses with maleic anhydride in ionic liquid. Biomacromolecules. 2010;**11:**3519–3524. DOI: 10.1021/bm1010118

[34] Sun YC, Xu JK, Xu F, Sun RC. Efficient separation and physico-chemical characterization of lignin from eucalyptus using ionic liquid–organic solvent and alkaline ethanol solvent. Industrial Crops and Products. 2013;**47:**277–285. DOI: 10.1016/j.indcrop.2013.03.025

[35] Wang Y, Song H, Hou JP, Jia CM, Yao S. Systematic isolation and utilization of lignocellulosic components from sugarcane bagasse. Separation Science and Technology. 2013;**48:**2217–2224. DOI: 10.1080/01496395.2013.791855

[36] Chen MJ, Zhang XQ, Liu CF, Sun RC, Lu FC. Approach to renewable lignocellulosic biomass film directly from bagasse. ACS Sustainable Chemistry & Engineering. 2014;**2:**1164–1168. DOI: 10.1021/sc400555v

[37] Liu CF, Sun RC, Qin MH, Zhang AP, Ren JL, Ye J, Luo W, Cao ZN. Succinoylation of sugarcane bagasse under ultrasound irradiation. Bioresource Technology. 2008;**99:**1465–1473. DOI: 10.1016/j.biortech.2007.01.062

[38] Lin Y, King JY, Karlen SD, Ralph J. Using 2D NMR spectroscopy to assess effects of UV radiation on cell wall chemistry during litter decomposition. Biogeochemistry. 2015;**125:**427–436. DOI: 10.1007/s10533-015-0132-1

[39] Guan Y, Zhang B, Qi XM, Peng F, Yao CL, Sun RC. Fractionation of bamboo hemicelluloses by graded saturated ammonium sulphate. Carbohydrate Polymers. 2015;**129:**201–207. DOI: 10.1016/j.carbpol.2015.04.042

[40] Sette M, Wechselberger R, Crestini C. Elucidation of lignin structure by quantitative 2D NMR. Chemistry–A European Journal. 2011;**17:**9529–9535. DOI: 10.1002/chem.201003045

[41] Wen JL, Yuan TQ, Sun SL, Xu F, Sun RC. Understanding the chemical transformations of lignin during ionic liquid pretreatment. Green Chemistry. 2014;**16:**181–190. DOI: 10.1039/c3gc41752b

[42] Kim JY, Shin EJ, Eom IY, Won K, Kim YH, Choi D, Choi IG, Choi JW. Structural features of lignin macromolecules extracted with ionic liquid from poplar wood. Bioresource Technology. 2011;**102:**9020–9025. DOI: 10.1016/j.biortech.2011.07.081

[43] Varanasi P, Singh P, Arora R, Adams PD, Auer M, Simmons BA, Singh S. Understanding changes in lignin of *Panicum virgatum* and *Eucalyptus globulus* as a function of ionic liquid pretreatment. Bioresource Technology. 2012;**126:**156–161. DOI: 10.1016/j.biortech.2012.08.070

[44] Wang HT, Yuan TQ, Meng LJ, She D, Geng ZC, Sun RC. Structural and thermal characterization of lauroylated hemicelluloses synthesized in an ionic liquid. Polymer Degradation and Stability. 2012;**97:**2323–2330. DOI: 10.1016/j.polymdegradstab.2012.07.033

IntechOpen